Pergamon

www.elsevier.com/locate/actaastro

PII: S0094-5765(02)00114-5

Acta Astronautica Vol. 51, No. 12, pp. 843–854, 2002

Printed in Great Britain
0094-5765/02/$ - see front matter

UNLOADING LAW FOR A LEO SPACECRAFT WITH TWO-GIMBALS SOLAR ARRAY

Y. W. JAN and J. C. CHIOU†

Department of Electrical and Control Engineering, National Chiao Tung University, HsinChu 30010, Taiwan

(Received 7 June 2000; accepted 3 January 2002)

Abstract—The purpose of this paper is to present a modified cross-product unloading law that can be used to provide an open-loop compensation control design to counteract the predominant effects of the gravity gradient torque. The modified cross-product unloading law, is successfully applied to a three-axis stabilized, nadir-pointed LEO spacecraft with two-gimbals solar array. The variation of the two solar array orientations can significantly change the spacecraft's moment of inertia during the nominal operation mode, which can produce significant momentum accumulation in the roll–yaw body plane and cause large yaw pointing error. A rigorous study of momentum management performance capability has been conducted by using a high-fidelity performance simulation software that contains models of four environmental disturbance torque (gravity gradient, aerodynamic, solar, and magnetic). The simulation results show that the proposed momentum unloading control law has enabled a substantial reduction in the maximum accumulated roll momentum, which results in improving the pointing accuracy of the LEO spacecraft enormously.

1. INTRODUCTION

For a three-axis stabilized spacecraft, the environmental disturbance torque is counteracted by an attitude control device, such as momentum wheels. The accumulated angular momentum is stored and when the device is saturated, it is usually unloaded by firing the reaction jets or using magnetic torquers. The penalty of using reaction jets includes fuel consumption, spacecraft disturbance, and contamination. Magnetic torquers are generally costly and have low control authority for large momentum dumping demand. The application of using the interaction between onboard magnets and the geomagnetic field for the attitude control of satellites [1–6] began in the early years of the space age. These research covered a wide spectrum of applications, including spin axis attitude control [1,2], spin speed control and nutation damping for spinning vehicles [2,3], and also magnetic control wheels for momentum exchange control or momentum wheels to provide pitch momentum bias [4,5]. A suboptimal solution is derived involving magnetic control to minimize the angular momentum stored in the reaction wheels, which in turn results in smaller wheels and reduced vibration levels [4]. Minimum energy desaturation Law (MEDL) [6] is designed to minimize the energy required to dump a given amount of momentum through the magnetic torquers during a given desaturation interval.

Stikler and Alfriend [5] proposed a closed-loop attitude control system for momentum bias spacecraft that performs the following functions: (1) initial acquisition, (2) nutation damping, (3) precession control, and (4) momentum bias regulation. The system is best suited for low-altitude, high-inclination, Earth-pointing momentum bias spacecraft. The system consists of three orthogonal electromagnets (mounted along the vehicle control axes), a three-axis magnetometer and a scan wheel.

1.1. Spacecraft architecture

In this paper, a LEO spacecraft which has two orthogonal drive axes for keeping solar arrays sun pointed during nominal mission operation was investigated in terms of the capability of momentum management. As illustrated in Fig. 1, the LEO spacecraft has a two-winged solar array where each wing can be rotated about two axes, alpha and beta, by stepper motors. When tracking the sun,

† Corresponding author. Tel.: +886-3-5731881; fax: +886-35-715-998.
E-mail address: chiou@cc.nctu.edu.tw (J. C. Chiou).

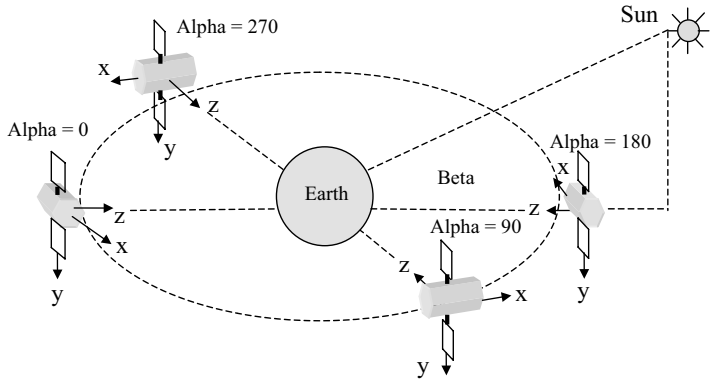

Fig. 1. Solar array rotation angles.

both the alpha and beta axes are controlled according to the onboard solar ephemeris calculation. The orbit is circular, inclined at 35°, and at 600 km altitude. During nominal mode, nadir pointing of the spacecraft is maintained with a wheeled based, pitch momentum bias (PMB) control system. The PMB control was selected due to design simplicity and reliability. There are two basic control methods, PMB and zero momentum bias (ZMB), which can be used for attitude control. The key difference between the PMB and ZMB systems is the way in which the spacecraft yaw attitude is controlled. Yaw pointing errors are controlled indirectly in a PMB system by limiting the accumulation of stored yaw momentum. In contrast, a typical ZMB system controls the yaw error directly with a dedicated yaw wheel. However, a yaw error signal has to be available continuously for this active control. An important characteristic of a PMB system is its high reliability. Operating a wheel above its bearing lift-off speed minimizes lubricant loss and the wear on ball bearings. The toughest environment for a wheel is to drive it at low speeds and in both directions. For a ZMB system, all three wheels are operated in this manner. Thus, long wheel life is a clear advantage of a PMB approach. The scan wheels utilized in the design provide the PMB and pitch/yaw control torques while they also provide the roll and pitch information by the attaching conical earth sensors. The selected approach for attitude control is the PMB method. The overriding consideration in this trade is design simplicity and reliability. Two wheels, an earth sensor and a sun sensor represent the minimum set of equipment.

The requirement of the attitude control accuracy for the nominal mode is 0.5° in roll, pitch and yaw axis, respectively. Attitude control system uses two scan wheels oriented in a "V" configuration, canted 20° from the pitch axis, as shown in Fig. 2, to produce the PMB along the negative *Y* spacecraft axis. This wheel configuration also provides the roll/yaw control loop for a two-axis momentum storage system [7]. Wheel speeds are automatically controlled with magnetic torque using the modified cross-product unloading law.

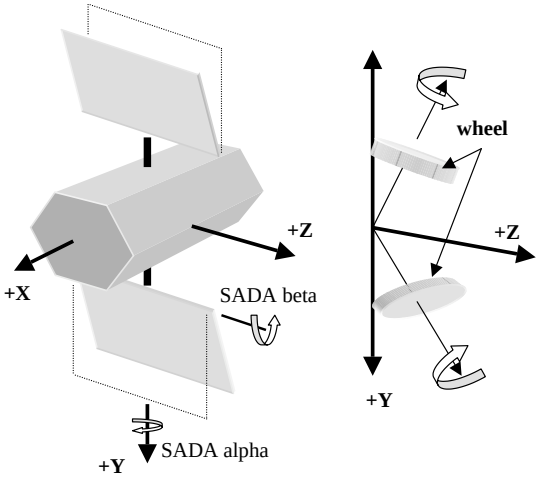

Fig. 2. Configuration of SADAs and wheels (solar arrays depicted by dash line are their null position, alpha = beta = 0°).

The spacecraft mass properties are a function of the solar array drive assembly (SADA) alpha (inner axis) and beta (outer axis) angles as shown in Fig. 2. Solar array rotations occur about two orthogonal axes. The inner rotation axis is nominally aligned parallel to the *Y* body axis and it remains fixed relative to the central spacecraft body. The outer rotation axis is nominally perpendicular to the inner rotation axis and it lies in the solar array plane. Potentiometer outputs of SADA are continuously read to provide both alpha and beta angles. In order to avoid the dynamic effect on the spacecraft

pointing, variable command patterns are used to slew the solar arrays, which decouple the dynamic resonance with the flexible mode of the spacecraft.

The major source of the stored environmental disturbance momentum is the gravity gradient torque due to the products of inertia induced in the spacecraft for large motions of the solar arrays about the beta SADA axis. Peak momentum accumulation rates in body axes due to the action of the aerodynamic, solar radiation pressure and magnetic disturbance torque are approximately an order of magnitude less than the peak momentum accumulation rates due to the gravity gradient torque.

1.2. Proposed unloading law

The baseline approach to magnetic momentum management was to employ the standard cross-product control law proposed by Stickler and Alfriend [5]. Stickler and Alfriend proposed a closed-loop attitude control system for momentum bias spacecraft that performs momentum bias regulation. Early analysis with the simulation in the study showed that their unloading approach would not be satisfactory for the LEO spacecraft which changes its moment of inertia due to the slewing of the two-axis solar arrays. The primary deterrent to the baseline approach was the large momentum accumulation rate from roll–yaw momentum due to the gravity gradient torque when the SADA beta angle was large.

Three improvements to the baseline approach were implemented in the paper:

1. Estimate the roll gravity gradient torque based on the knowledge of the SADA alpha and beta angles in order to generate the open-loop magnetic torque compensation to counteract the roll gravity gradient torque. Analysis shows that the open-loop compensation effectively counteracts the high rate of roll–yaw momentum accumulation while introducing extra disturbance momentum accumulation in the spacecraft pitch axis. Yaw pointing is improved because the roll–yaw momentum is better managed. Net accumulation of pitch momentum is maintained within acceptable limits by the standard cross-product unloading law.
2. Estimate the roll spacecraft momentum based on yaw error information. Since the scan wheel speeds provide no roll momentum information, the baseline approach was to leave the roll element of the vector of the momentum to be unloaded to zero. Unloading performance can be significantly enhanced by providing roll momentum information. The simulation results shown in this paper is based on the assumption that we have the full knowledge of the accumulated roll momentum which, of course, is unrealistic. However, an estimation of the roll momentum can be made from the flight software processing. The present estimation of the roll momentum to be unloaded is

$$H_{\text{dump}}(x) = \psi H_{\text{B}}, \tag{1}$$

where H_{B} is the value of the PMB and ψ is the yaw error calculated by the onboard flight software.
3. Provide integral compensation to drive the mean value of the net accumulated momentum in each spacecraft axis to zero. Driving the mean net accumulated momentum to zero tends to lower the peak values.

This paper is organized as follows. Section 2 summarizes the mathematical model used to calculate disturbance torque values and discusses disturbance torque characteristics for the LEO satellite. The design of the magnetic control law for momentum management is given in Section 3. Results of the momentum unloading system performance are given in Section 4.

2. ENVIRONMENTAL DISTURBANCE TORQUE MODELS

A high-fidelity simulator was developed to perform the simulation for the study. The simulator contains models of four environmental disturbance torque (gravity gradient, aerodynamic, solar, and magnetic) and can simulate both perfect nadir pointing for the nominal mission mode, and inertial pointing. The program was used to evaluate momentum unloading performance in nominal mission mode over long time periods, usually of 90 days or more. The four environmental disturbance torque models included in the program are summarized in the following four subsections.

2.1. Gravity gradient torque

The equation used to evaluate the gravity gradient torque about the spacecraft center of gravity (c.g.) is taken from Wertz [8]:

$$\tau_{\text{GG}} = \frac{3\mu}{R_{\text{S}}^3}[\mathbf{R}_{\text{S}} \times (\mathbf{I} \cdot \mathbf{R})]. \tag{2}$$

The parameters of eqn. (2) are summarized in Table 1. Equation (2) may be expanded to provide

Table 1. Parameter values used for gravity gradient model

Parameter	Description	Value
μ	Earth's gravitational constant	398600.5
R_S	Distance from geocenter to spacecraft c.g. (km)	Orbital altitude + 6378.0
$\mathbf{R}_S$	Unit vector pointing from the spacecraft c.g. to geocenter (expressed in spacecraft body coordinates)	[0, 0, 1] for nadir pointing; varies with orbit for inertial pointing
$\bar{I}$	Spacecraft inertia matrix about c.g. (kg m^2) Deployed configuration	See Table 2 for representative values of the inertia matrix

Table 2. Variations in the spacecraft inertia matrix for selected SADA angles

SADA positions	Alpha = 0°	Alpha = 90°
Beta = 0°	$\begin{bmatrix} 142 & -0.7 & 2 \\ -0.7 & 102 & 4.6 \\ 2 & 4.6 & 224 \end{bmatrix}$	$\begin{bmatrix} 110 & 4.4 & 2 \\ 4.4 & 134 & -0.4 \\ 2 & -0.4 & 221 \end{bmatrix}$
Beta = −35°	$\begin{bmatrix} 140 & -0.7 & 17 \\ -0.7 & 134 & 53.1 \\ 17 & 53.1 & 192 \end{bmatrix}$	$\begin{bmatrix} 110 & 52.8 & 2 \\ 52.8 & 134 & -0.4 \\ 2 & -0.4 & 200 \end{bmatrix}$

greater insight into the nature of the gravity gradient torque, and its relationship to the spacecraft mass properties is given as follows:

$$\tau_{GG} = \frac{3\mu}{R_S^3} \begin{bmatrix} (I_{zz} - I_{yy})R_yR_z - I_{xy}R_xR_z + I_{yz}(R_y^2 - R_z^2) + I_{xz}R_xR_y \\ (I_{xx} - I_{zz})R_xR_z + I_{xy}R_yR_z + I_{xz}(R_z^2 - R_x^2) - I_{yz}R_xR_y \\ (I_{yy} - I_{xx})R_xR_y + I_{yz}R_xR_z + I_{xz}(R_x^2 - R_y^2) - I_{xz}R_yR_z \end{bmatrix} \quad (3)$$

For nominal mission, the simulation assumes that the spacecraft is perfectly nadir pointed. That is, $R_x = 0, R_y = 0, R_z = 1$. The spacecraft mass properties are a function of the SADA alpha (inner axis) and beta (outer axis) angles. For large beta angles, large products of inertia are produced. The present analysis has assumed the limits of the SADA beta angle to be at $\pm 35^\circ$. Plots of I_{yz} and I_{xz} versus time would show sinusoids varying at the orbital frequency. The plots of I_{xy} and I_{yz} would have approximately equal amplitudes but would be 90° (1/4 orbit) out of phase. Typical spacecraft inertia tensors for selected SADA alpha and beta angles are shown in Table 2.

In nominal mission with perfect nadir pointing, the gravity gradient torque effects, due to the differences of the moments of inertia I_{xx}, I_{yy} and I_{zz}, are zero. With the SADA beta axis limited to very small angles, the products of inertia are also small and the gravity gradient disturbance torque is relatively benign. The most pertinent terms of the gravity gradient torque are due to the large products of inertia I_{yz} when the solar arrays are moved to large angles in the SADA beta axis. I_{yz} produces a large cyclic roll (x-axis) body torque with an amplitude of 1.9×10^{-4} N m. The pitch body torque is cyclic in body axes with an amplitude of 6.0×10^{-5} N m. Although the roll gravity gradient torque is cyclic in body axes, it has a very large secular component in inertial axes and produces significant momentum accumulation in the roll–yaw body plane. The gravity gradient momentum accumulation rate in the roll–yaw body plane may be as high as 8 N m s/day. This momentum must be quickly unloaded to avoid large yaw pointing errors in the LEO spacecraft PMB control approach.

2.2. Aerodynamic torque

The aerodynamic disturbance torque model presented in this paper is based on a surface model of the physical shape of the LEO spacecraft. The surfaces, which are all plates, used in the aerodynamic model are summarized in Table 3. The model consists of six flat rectangular plates for the hexagonal spacecraft "box", two hexagonal endplates and four flat rectangular plates representing the solar arrays (each solar array has a front and a back plate).

The physical parameters used in each plate are defined in terms of its area A and an inward pointing unit normal $\mathbf{N}$. The location of each plate is defined by the vector r_S, the position of the centroid of the plate with respect to the spacecraft c.g. The spacecraft c.g. is calculated from the mass properties of the spacecraft bus without the solar arrays, the mass properties of the solar arrays, and the position of the solar arrays. In this paper, we

Table 3. Plate model of the LEO spacecraft used to calculate aerodynamic and solar radiation pressure environmental disturbance torque

		Inward unit normal			Center of surface, r_S			Radiation coefficients	
Surface	Area (m^2)	N_x	N_y	N_z	r_{sx}(m)	r_{sy}(m)	r_{sz}(m)	σ_A	σ_D
RAM platform	0.58	−1.0	0.0	0.0	1.09	0.0	0.0	0.2	1.0
Wake platform	0.58	1.0	0.0	0.0	0.0	0.0	0.0	0.2	1.0
$+Y/+Z$ panel	0.51	0.0	−0.5	−0.866	0.55	0.21	0.36	0.20	1.0
$+Y$ panel	0.51	0.0	−1.0	0.0	0.55	0.41	0.00	0.20	1.0
$+Y/-Z$ panel	0.51	0.0	−0.5	0.866	0.55	0.21	−0.36	0.20	1.0
$-Y/-Z$ panel	0.51	0.0	0.5	0.866	0.55	−0.21	−0.36	0.20	1.0
$-Y$ panel	0.51	0.0	1.0	0.0	0.55	−0.41	0.0	0.20	1.0
$-Y/+Z$ panel	0.51	0.0	0.5	−0.866	0.55	−0.21	0.36	0.20	1.0
$+Y$ S/A Sun	2.83	0.0	0.0	−1.0	0.58	2.32	−0.10	0.72	1.0
$+Y$ S/A shade	2.83	0.0	0.0	1.0	0.58	2.32	−0.10	0.20	1.0
$-Y$ S/A Sun	2.83	0.0	0.0	−1.0	0.58	−2.32	0.10	0.72	1.0
$-Y$ S/A shade	2.83	0.0	0.0	1.0	0.58	−2.32	0.10	0.20	1.0

Table 4. Parameter values used for the aerodynamics torque model

Parameter	Description	Value
ρ	Atmospheric density (kg/m^3)	Calculated using a Jacchia Atmospheric Density model
f_T	Tangential accommodation coefficient	1.0
f_N	Normal accommodation coefficient	1.0
v	Speed of the impinging particle flow (m/s)	Orbit dependent, nominally 7558 m/s
V	Unit vector in the direction of the impinging particle flow expressed in spacecraft body coordinates	Tangent to (circular) orbit

assume a "balanced" solar array configuration that does not cause variation of the spacecraft c.g. due to array motion. The spacecraft c.g. is calculated to be

$$\text{c.g.} = (1, 0.005, 0.01)\ \text{m}.$$

The solar arrays are always assumed to be sun pointed and subjected to a beta axis travel restriction of $\pm 35^\circ$. The solar array data of Table 3 indicates the nominal array data for the arrays in the null position of alpha $= 0^\circ$ and beta $= 0^\circ$.

The mathematical model of the aerodynamic disturbance torque is given by a set of equations taken from Ref. [8]:

$$\tau_{\text{aero}} = \sum_{\text{surfaces}} r_S \times f_{\text{aero}}, \tag{4}$$

where f_{aero} is the force acting on each surface. For the flat plates,

$$f_{\text{aero}} = 2[\tfrac{1}{2}\rho v^2]A(\mathbf{N}\cdot\mathbf{V})[f_T v + (2 - f_T - f_N)(\mathbf{N}\cdot\mathbf{V})\mathbf{N}] \quad \text{for } (\mathbf{N}\cdot\mathbf{V}) > 0, \tag{5}$$

$$f_{\text{aero}} = 0 \quad \text{for } (\mathbf{N}\cdot\mathbf{V}) \leqslant 0, \tag{6}$$

where the undefined parameters for Eqs. (5) and (6) are summarized in Table 4. Note that for the choice of $f_T = f_N = 1$, there is no lift component for the aerodynamic force. The value of the atmospheric density was calculated using a Jacchia atmospheric density model. The value of the atmospheric density ranged from 0.5×10^{-12} to 2.4×10^{-12} kg/m^3.

The aerodynamic torque is the smallest environmental disturbance torque acting on the LEO spacecraft at its nominal 600 km circular orbit. Aerodynamic torque will increase at lower altitudes. Relatively conservative solar activity parameters were used in this study to generate conservatively high values of the aerodynamic density using the Jacchia atmospheric density model. The body yaw component is the most significant portion of the disturbance, it reaches the values of 2.3×10^{-6} N m.

2.3. Solar torque

The solar disturbance torque model also uses the spacecraft plate model described in Table 3. In addition to the physical descriptions shown in Table 3, the solar model assigns to each surface an absorption coefficient σ_A and a diffuse reflectivity coefficient σ_D. The parameters values for σ_A and σ_D listed in Table 3 are standard values for white painted surfaces and solar array photo cells. The two coefficients correspond to the three coefficients

C_a, C_d and C_s of Wertz [8] as follows:

$$C_a = \sigma_A, \quad 0 \leqslant \sigma_A \leqslant 1, \tag{7}$$

$$C_d = \sigma_d(1 - \sigma_A), \quad 0 \leqslant \sigma_D \leqslant 1, \tag{8}$$

$$C_s = (1 - \sigma_D)(1 - \sigma_A), \tag{9}$$

where C_a is the absorption coefficient, C_d is the coefficient of diffuse reflection, and C_s is the coefficient of specular reflection. The sum of these three coefficients should equal to unity,

$$C_a + C_d + C_s = 1. \tag{10}$$

The solar radiation force acting on each plate is determined by

$$f_{solar} = PA(\mathbf{N} \cdot \mathbf{S})\{(C_a + C_d)\mathbf{S} + [\tfrac{2}{3}C_d + 2C_s(\mathbf{N} \cdot \mathbf{S})\mathbf{N}]\}, \tag{11}$$

where $\mathbf{S}$ is the unit vector from the sun to the spacecraft and $\mathbf{N}$ is the inward pointing unit normal of the plate. The solar torque for the spacecraft is then calculated by

$$\tau_{solar} = \sum_{surfaces} r_S \times f_{solar}, \tag{12}$$

where r_S is the vector from the spacecraft center of gravity to the centroid of the current plate. No shading is included in the solar torque model. Note that the shading is not considered to be significant in the calculation of the solar torque. The value of the maximum solar torque is in the order of 9.0×10^{-6} N m.

2.4. Magnetic torque

The source of the magnetic disturbance torque is coming from the residual magnetic moment of the spacecraft moving through the earth's magnetic field. The torque is easy to calculate once the residual magnetic moment and the strength of the magnetic field at the spacecraft are known. The equation describing the torque is

$$\tau_{mag} = m \times B, \tag{13}$$

where B is the magnetic field vector in T and m is the residual spacecraft magnetic dipole moment in A m^2.

The value of the spacecraft residual magnetic moment being used in the magnetic disturbance torque model is 1.0 A m^2 per spacecraft axis. This value is determined based on the typical engineering experience. The sign of the residual magnetic moment in each spacecraft axis has been arbitrarily assigned. The RSS of the residual spacecraft magnetic dipole moment used in this momentum management analysis is 1.73 A m^2.

The magnetic field model used in the simulation has the same accuracy as the eight-order spherical dipole model documented in Appendix H of Ref. [8]. Typical magnitudes of the magnetic field at the nominal mission orbit of the LEO spacecraft range from 0.18 to 0.45 G (18–45 μT). The peak magnitude of the magnetic disturbance torque due to the residual spacecraft dipole moment is 4.5×10^{-5} N m.

3. MOMENTUM MANAGEMENT CONTROL LAW

A block diagram of the control system is shown in Fig. 3. The procedures of the unloading system are described as follows:

(1) The residual momentum, H_{res}, to be unloaded is calculated from the deviations of the wheel speeds from bias wheel speeds. The wheel speeds are provided by the built-in tachometers. This gives the pitch and yaw values of Hres since the wheel spin axes are all located in the pitch yaw plane.

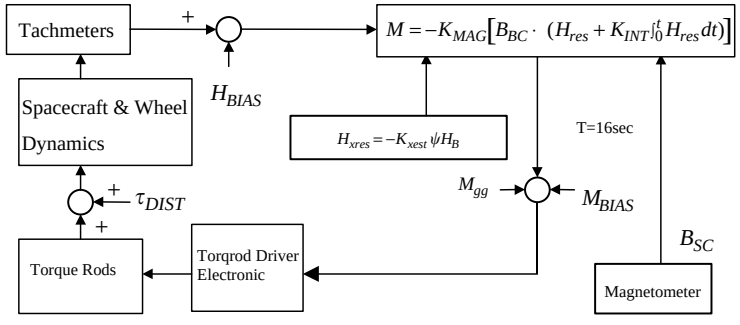

Fig. 3. Momentum management block diagram.

(2) The roll residual momentum is calculated from the yaw attitude error that is propagated onboard using the gyros. $H_{\text{res}}(x)$ is equal to yaw error times the PMB H_{B}.

(3) An open-loop gravity gradient compensation term is calculated based on the solar array positions. This term is added to the basic cross-product torque rod command.

(4) An integral term is used to help center the positive and negative peaks of the residual momentum command about zero.

(5) The residual momentum is used in a traditional cross-product unloading law to generate basic torque rod commands.

Table 5. Peak net accumulated momentum in body axes for a 90-day run beginning at winter solstice with the spacecraft in the nominal nadir-pointed mission orientation

Axis	Maximum net momentum accumulation in body axes (N m s) (N m s)	Torque rod duty cycle in body axes (60-day Average) (%)
X	0.055	7.2
Y	0.110	7.7
Z	0.080	9.4

The LEO spacecraft momentum management control law now takes the form

$$M = M_{\text{cp}} + M_{\text{gg}}, \tag{14}$$

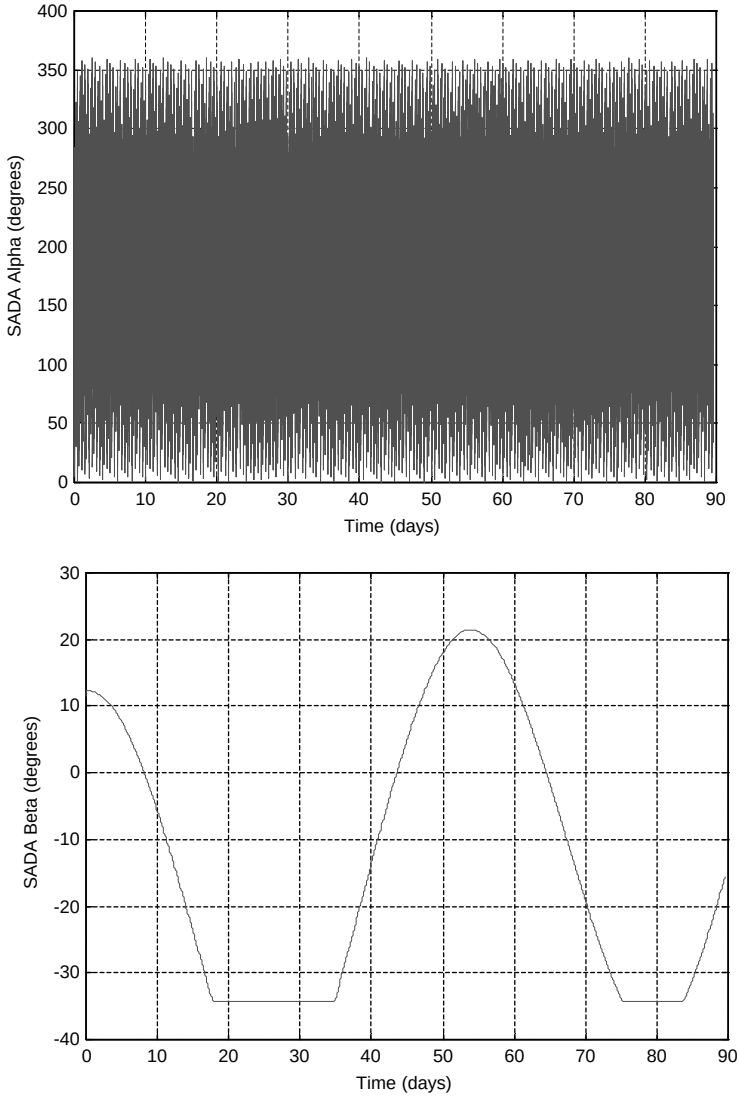

Fig. 4. SADA alpha, SADA beta variations over 90 days beginning at winter solstice with a right ascension of 0°. High-frequency variations are at orbit rate.

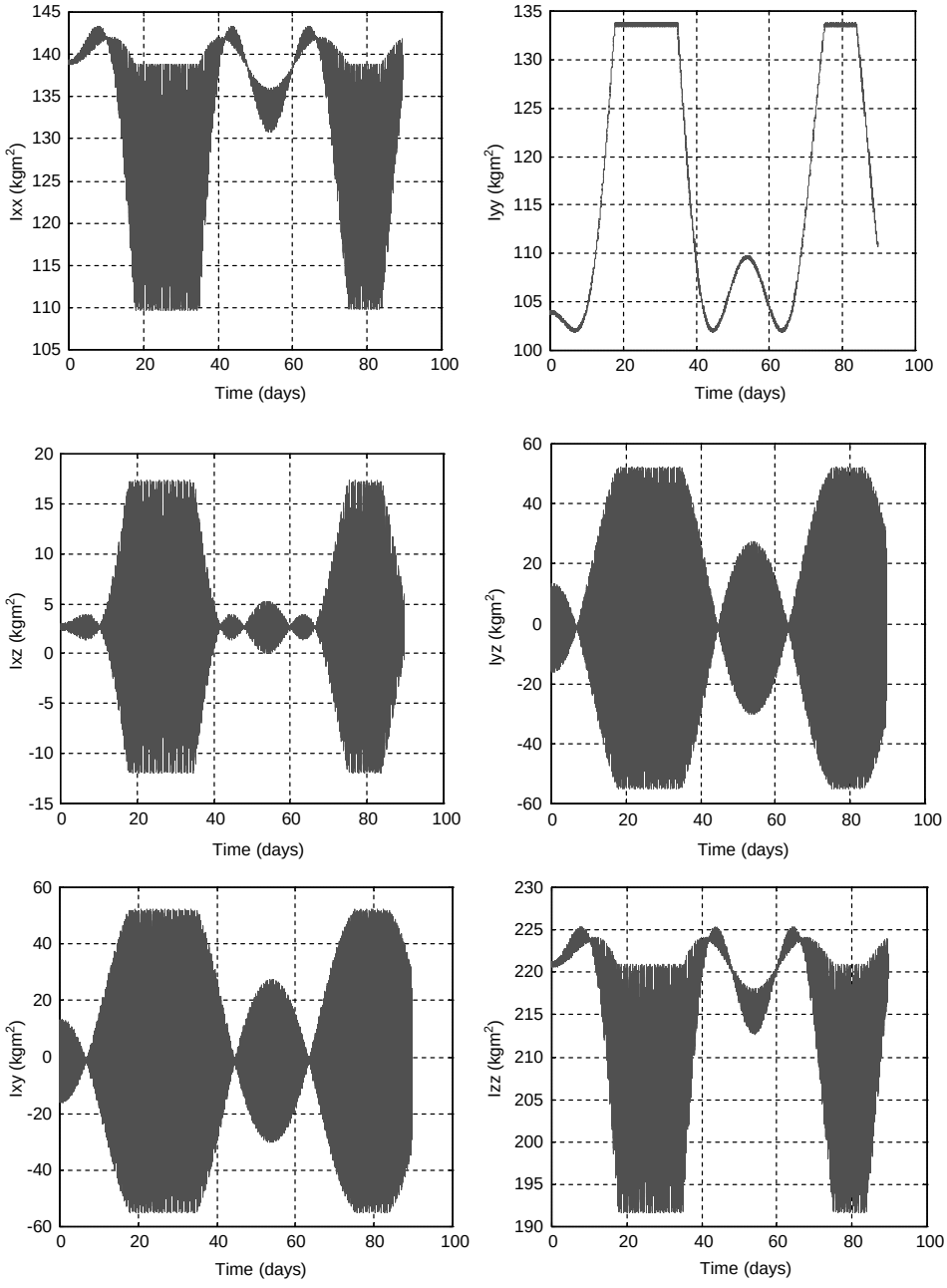

Fig. 5. Spacecraft mass property variation over 90 days beginning at winter solstice with a right ascension of 0°. High-frequency variations are at orbit rate.

where M_{cp} is due to the modified cross-product law and M_{gg} is the open-loop term used to cancel the estimated effects of the roll–yaw gravity gradient torque. M_{cp} is calculated as

$$M_{cp} = -K_{mag}(B \times H_{dump}) \tag{15}$$

with

$$H_{dump} = H_{res} + K_{ol} \int_0^t H_{res}\, dt. \tag{16}$$

A pseudo-inverse is used to calculate M_{gg}. The starting point of the procedure is the magnetic torque equation

$$\tau_{des} = M_{gg} \times B = \begin{bmatrix} 0 & B_z & -B_y \\ -B_z & 0 & B_x \\ B_y & -B_x & 0 \end{bmatrix} \begin{bmatrix} M_{ggx} \\ M_{ggy} \\ M_{ggz} \end{bmatrix}. \tag{17}$$

In particular, we would like τ_{des} to cancel the roll–yaw gravity gradient torque (ideally, we

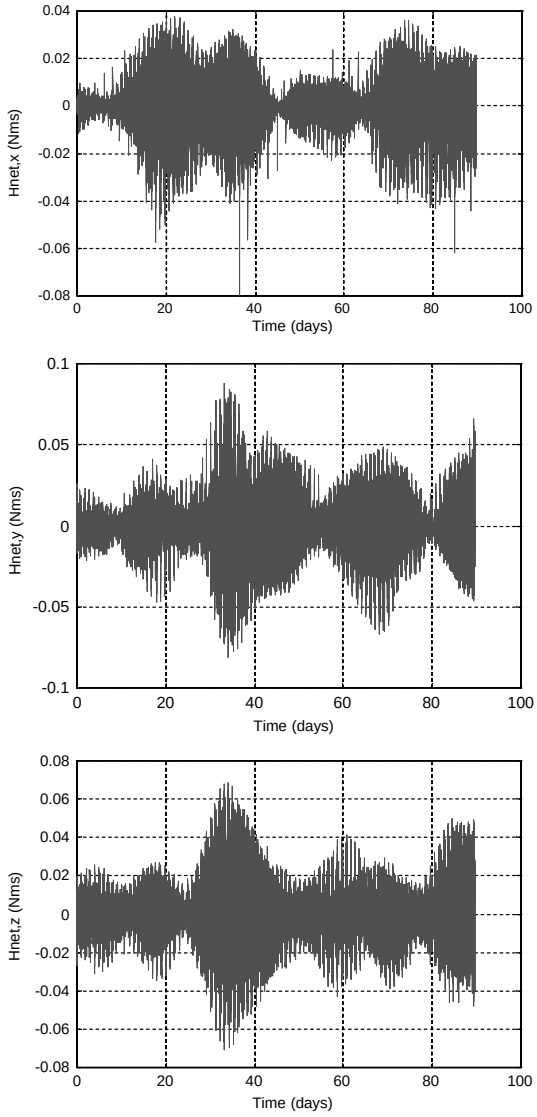

Fig. 6. Net accumulated momentum in body axes over 90 days beginning at winter solstice with a right ascension of 0°.

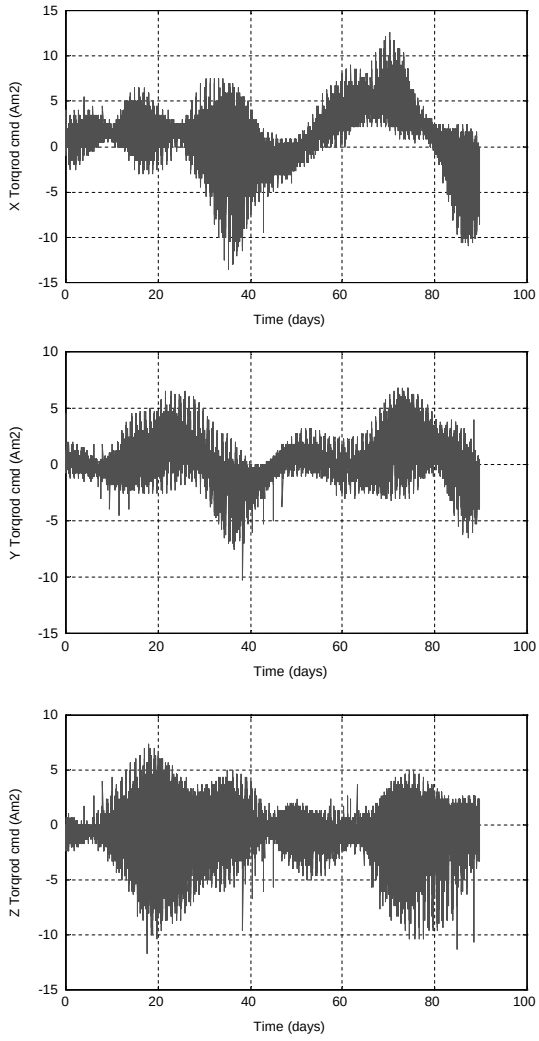

Fig. 7. Commanded torque rod moments over 90 days beginning at winter solstice with a right ascension of 0°.

would like to cancel all components of the gravity gradient torque, but this is not possible),

$$\tau_{\text{des}} = -\tau_{\text{GG}} = \begin{bmatrix} \tau_{\text{gg}x'} \\ \tau_{\text{gg}z} \end{bmatrix}. \tag{18}$$

Note that M_{gg} is solved by

$$M_{\text{gg}} = (B_{\text{red}})^{-1}\tau_{\text{des}}, \tag{19}$$

where

$$(B_{\text{red}})^{-1} = \begin{bmatrix} 0 & B_z & -B_y \\ B_y & -B_x & 0 \end{bmatrix}^{-1} = B_{\text{red}}^{\text{T}}(B_{\text{red}}B_{\text{red}}^{\text{T}})^{-1} \tag{20}$$

is the (right) pseudo-inverse of the 2×3 (reduced magnetic field) matrix B_{red}. Ideally, the above-mentioned open-loop compensation provides a torque generated by the calculated magnetic moment that would exactly oppose the roll–yaw gravity gradient torque. In practice, however, τ_{des} is only an estimation of the true gravity gradient torque and cancellation will not be exact. The roll gravity gradient torque is estimated as

$$\tau_{\text{gg}x} = A_{\text{bb}} + B_{\text{gg}} \sin\alpha \sin\beta \cos\beta, \tag{21}$$

where α and β are the SADA alpha and beta axis positions. Little effort is required to adjust A_{gg} and B_{gg} so that the residual roll gravity gradient torque is less than 1.0×10^{-5} N m. Since for the nadir pointed nominal mode mission, the yaw component of the gravity gradient torque is nearly zero, $\tau_{\text{gg}z}$ is set to be at zero.

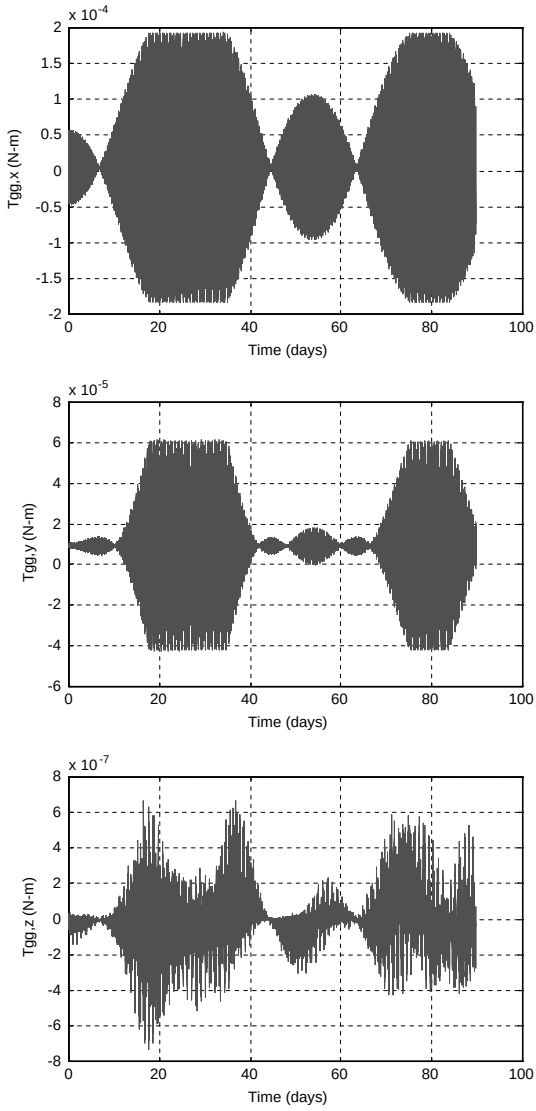

Fig. 8. Gravity gradient disturbance torques in body axes over 90 days beginning at winter solstice with a right ascension of 0°.

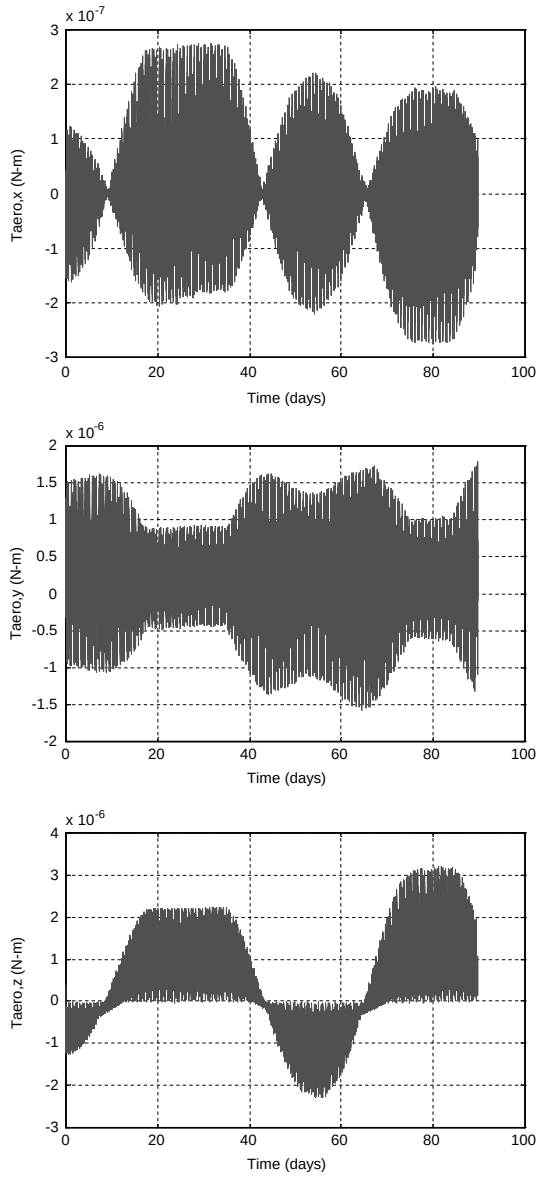

Fig. 9. Aerodynamic disturbance torques in body axes over 90 days beginning at winter solstice with a right ascension of 0°.

4. MOMENTUM UNLOADING PERFORMANCE

Momentum unloading performance was evaluated in the nominal nadir pointing mission. All runs use three magnetic torque values at 20 A m^2 and oriented along the spacecraft X-, Y- and Z-axis.

Due to the high nodal regression rate (nearly 6°/day), there seemed to be no strong seasonal dependence on the action of the four environmental disturbance torque. Much more critical to the action of the disturbance torque are the orbit beta angle (the angle between the sun line and the orbit plane) and the changes that result in the spacecraft inertia matrix as the SADAs track the sun. The present analysis assumed a limit on the maximum travel about the SADA beta axis to be $\pm 35^\circ$.

Overall variations in the performance of the momentum unloading over the 90-day runs were not significant. The best momentum unloading performance occurs when the SADA beta angles, and the resulting products of inertia, are small. The highest residual momentum are consistently recorded when the SADA beta angles are near their 35° limits. Results for the winter 90-day case (the worst case) are presented in Table 5.

Plots for the 90 days nominal mission case that began at winter solstice are attached. Fig. 4 shows orbital and long-term variations in the alpha and beta SADA angles. Also shown in Fig. 4 are the true

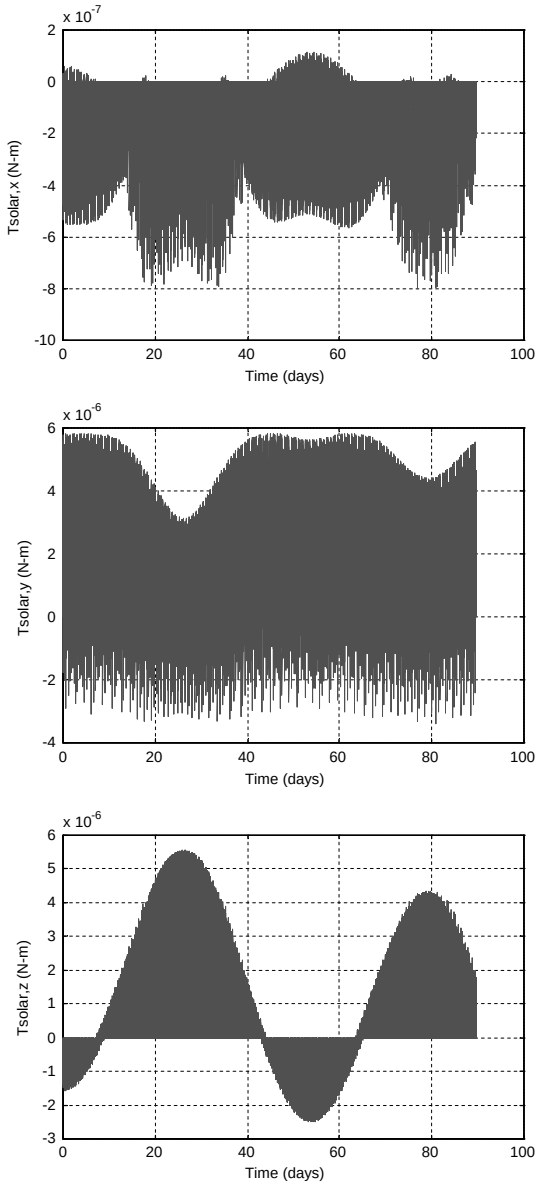

Fig. 10. Solar radiation pressure disturbance torques in body axes over 90 days beginning at winter solstice with a right ascension of 0°.

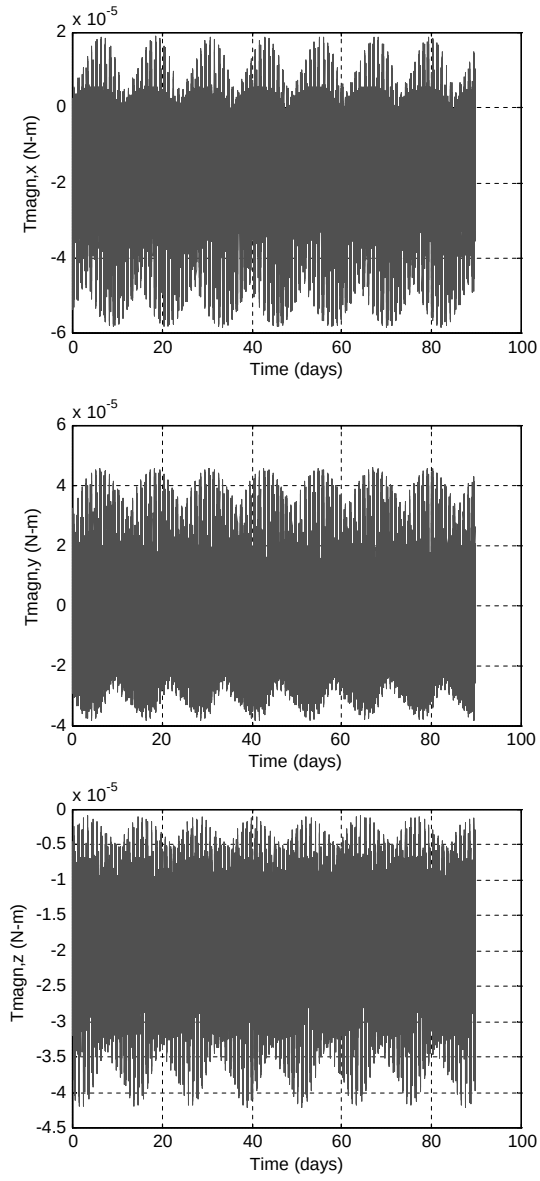

Fig. 11. Magnetic disturbance torques in body axes over 90 days beginning at winter solstice with a right ascension of 0°.

beta angle and the solar array pointing error as the SADA beta angle is limited to 35°. Figure 5 shows the corresponding variations in the spacecraft mass properties. The high-frequency variations are at orbit rate, the slower variations are correlated to the SADA beta angle.

Figure 6 shows the net accumulated momentum in each of the three body axes. Clearly the peak accumulations correspond to times where the SADA beta angle is near or at its limit. The commanded magnetic moment for each of the three torque rods is shown in Fig. 7. The final limitation on unloading performance is seen not to be torque rod size (as the duty cycles are relatively low), but rather geometric difficulties in certain regions of the orbit where the momentum to be unloaded and the magnetic field are nearly in line.

Plots for the disturbance torque in body axes for this case are shown in Figs. 8–11: the gravity gradient torque in Fig. 8, the aerodynamic torque in Fig. 9, the solar radiation pressure torque in Fig. 10, and the magnetic disturbance torque in Fig. 11.

The pointing performance for roll, pitch and yaw errors are shown in Fig. 12. As they can be seen, the attitude errors are controlled within the pointing

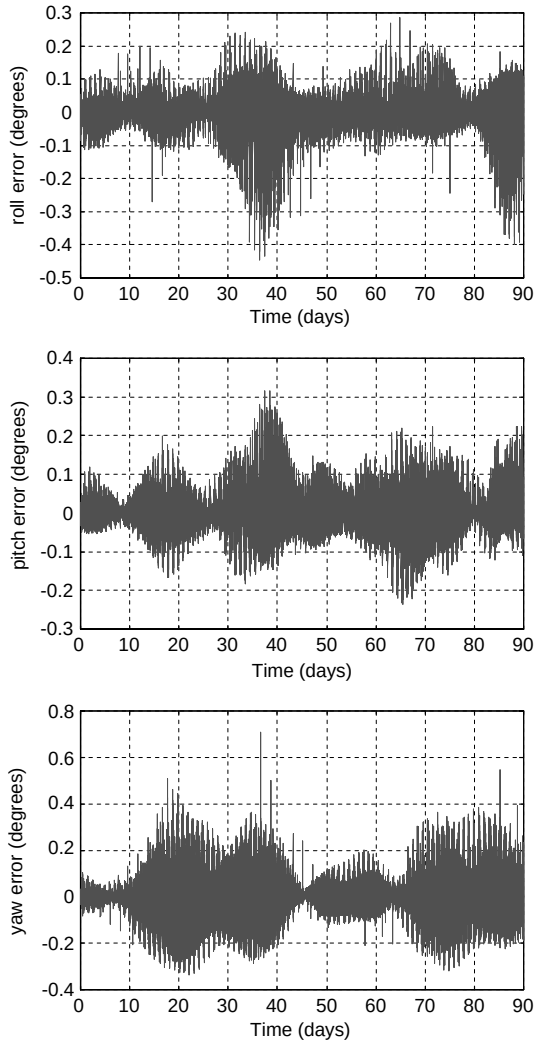

Fig. 12. Pointing accuracy over 90 days beginning at winter solstice with a right ascension of 0°.

requirement of 0.5° for all three axes. Since the nominal pitch momentum bias of the LEO spacecraft is 6.2 N m s, the peak roll accumulated momentum of 0.055 N m s as shown in Fig. 6 will cause a yaw pointing error of 0.51°. This pointing error occurs once per orbit while the SADA beta angle is at its 35° limit. For lower SADA beta angles, momentum unloading performance is improved and the simulation result shows that the yaw pointing requirement of 0.5° can generally be met.

5. CONCLUSION

A modified cross-product unloading law which provides an open-loop compensation term designed to counteract the predominant effects of the gravity gradient torque produced by large SADA beta angle is developed. The effect of using the residual roll momentum compensation term is to increase the overall efficiency of the unloading because the unloading of residual roll/yaw momentum takes place around the entire orbit. The momentum management performance capability has been proved by using a detailed performance simulation that contains models of four environmental disturbance torque (gravity gradient, aerodynamic, solar, and magnetic). The simulation results show that the modified momentum unloading control law has effectively improved the pointing accuracy of the spacecraft with two-axis solar arrays slewing.

REFERENCES

1. Alfriend, K. T. and Lindberg, R. E. Geomagnetic field effects on the design of a magnetic attitude control system. *Journal of the Astronautical Science*, 1979, **XXVII**, 269–292.
2. Renard, M. L., Command laws for magnetic attitude control of spin-stabilized Earth satellites. *Journal of Spacecraft*, 1996, **4**(2), 156–163.
3. Wheeler, P. C., Spinning spacecraft attitude control via the environmental magnetic field. *Journal of Spacecraft*, 1967, **4**(12), 1631–1637.
4. Wernli, A., Minimization of reaction wheel momentum storage with magnetic torque. *Journal of the Astronautical Sciences*, 1978, **XXVI**(3), 257–278.
5. Stickler, A. C. and Alfriend, K. T., Elementary magnetic attitude control system. *Journal of Spacecraft and Rockets*, 1976, **13**(5), 282–287.
6. Glaese, I. R., Kennel, H. F., Nurre, G. S., Seltzer, S. M. and Shelton, H. L., A low cost LST pointing control system, AIAA Paper No. 75-1057, August (1975) 20–22.
7. Lebsock, K. L., High pointing accuracy with a momentum bias attitude control system. *Journal of Guidance and Control*, 1980, **3**(3), 1952–1202.
8. Wertz, J. R., *Spacecraft Attitude Determination and Control*, Kluwer Academic Publishers, Boston, 1990.